Ultrafast X-Ray Scattering Measurements of Coherent Structural Dynamics on the Ground-State Potential Energy Surface of a Diplatinum Molecule

Kristoffer Haldrup, Gianluca Levi, Elisa Biasin, Peter Vester, Mads Goldschmidt Laursen, Frederik Beyer, Kasper Skov Kjær, Tim Brandt van Driel, Tobias Harlang, Asmus O. Dohn, Robert J. Hartsock, Silke Nelson, James M. Glownia, Henrik T. Lemke, Morten Christensen, Kelly J. Gaffney, Niels E. Henriksen, Klaus B. Møller, and Martin M. Nielsen

Ultrafast X-ray scattering measurements of coherent structural dynamics on the ground-state potential energy surface of a diplatinum molecule

Kristoffer Haldrup,[1] Gianluca Levi,[2, 3] Elisa Biasin,[1, 4] Peter Vester,[1] Mads Goldschmidt Laursen,[1] Frederik Beyer,[1] Kasper Skov Kjær,[1, 5, 4] Tim Brandt van Driel,[1, 6] Tobias Harlang,[1, 5] Asmus O. Dohn,[2, 7] Robert J. Hartsock,[4] Silke Nelson,[6] James M. Glownia,[6] Henrik T. Lemke,[6, 8] Morten Christensen,[1] Kelly J. Gaffney,[4] Niels E. Henriksen,[2] Klaus B. Møller,[2] and Martin M. Nielsen[1]

[1] *Technical University of Denmark, Department of Physics,*
Fysikvej 307, DK-2800 Kongens Lyngby, Denmark.
[2] *Technical University of Denmark, Department of Chemistry,*
Kemitorvet 207, DK-2800 Kongens Lyngby, Denmark.
[3] *Current address: Science Institute of the University of Iceland, VR-III, 107 Reykjavik, Iceland*
[4] *PULSE Institute, SLAC National Accelerator Laboratory, Menlo Park, California 94025, USA*
[5] *Department of Chemical Physics, Lund University, Box 118, S-22100 Lund, Sweden*
[6] *LCLS, SLAC National Accelerator Laboratory, Menlo Park, California 94025, USA*
[7] *Science Institute of the University of Iceland, VR-III, 107 Reykjavik, Iceland*
[8] *SwissFEL, Paul Scherrer Institut, 5232 Villigen PSI, Switzerland*

We report XFEL experiments addressing ground-state structural dynamics of the di-platinum anion Pt_2POP_4 following photoexcitation. The structural dynamics are tracked with <100 femtosecond time resolution by X-ray scattering, utilizing the anisotropic component to suppress contributions from the bulk solvent. The X-ray data exhibits a strong oscillatory component with period $T = 0.28$ picoseconds and decay time 2.2 picoseconds, and structural analysis of the difference signal directly shows this as arising from ground-state dynamics along the PtPt coordinate. The results are compared with QM/MM BOMD simulations and demonstrate how off-resonance excitation can be used to prepare a vibrationally cold excited-state population complemented by a structure-dependent depletion of the ground-state population which subsequently evolves in time, allowing direct tracking of ground-state structural dynamics.

Optical lasers with femtosecond pulse lengths have enabled a host of studies of the excited-state kinetics and dynamics. With the arrival of X-ray and electron sources with pulse lengths in the sub-picosecond regime, the bond-length and -angle dynamics of the photoexcited molecules can now be directly measured [1–3]. However, the majority of chemical reactions take place between molecular species in their electronic ground states and the energy landscape of ground-state molecules is therefore of fundamental interest. The dynamics of ground-state molecules have mainly been investigated through time-resolved optical methods based on preparing non-equilibrium, coherent vibrational states through combined absorption and Raman processes involving an excited-state potential surface. This is today a mature field spanning several methodologies, e.g. Resonant Impulsive Stimulated Raman Scattering (RISRS) and Coherent Anti-Stokes Raman scattering (CARS) [4–8]. These spectroscopy methods provide a powerful approach to characterizing vibrational eigenfrequencies for harmonic modes, but do not directly access bond lengths and angles. Similar limitations apply to the so-called *Lochfrass* or 'R-dependent ionization' spectroscopies, where the ground state is selectively depleted as a function of some key structural parameter [9–12].

The reliance on indirect, albeit powerful, spectroscopic methods to probe the potential energy landscape of ground-state molecules has been due to a lack of structurally-sensitive probes with the requisite time resolution. Here we show how hard X-ray Free Electron Laser (XFEL) sources [13] now make it possible to directly map the structural dynamics of an ensemble of molecules as it evolves on the ground-state potential surface. illustrating this approach we investigate how the ground-state population of the much-studied di-platinum anion Pt-POP $[Pt_2(P_2O_5H_2)_4]^{4-}$ (Figure 1) [14–23] evolves following Pt-Pt distance-dependent photo-depletion of the ground-state population.

Our structural analysis of the X-ray data is compared with Born-Oppenheimer Molecular Dynamics (BOMD) simulations using quantum mechanics/molecular mechanics (QM/MM) calculated forces [24–26]. Following Fleming and co-workers [72], the simulations are used to model the dynamics of a ground-state non-equilibrium density created by the pump pulse through propagation of a so-called hole in the classical ground-state equilibrium distribution mirroring at time zero the distribution promoted to the excited state. The ground-state dynamics predicted this way becomes increasingly accurate in the high temperature limit ($T >> \Theta$, where $\Theta = h\nu/k_B$ is the vibrational temperature) as more vibrational levels of the ground state are initially populated (for PtPOP the ground-state vibrational temperature is 170 K giving a vibrational excitation fraction [28] of $\approx$0.6 at 300 K).

The photophysics of PtPOP have been studied for four decades [22] and it is well established that excitation in
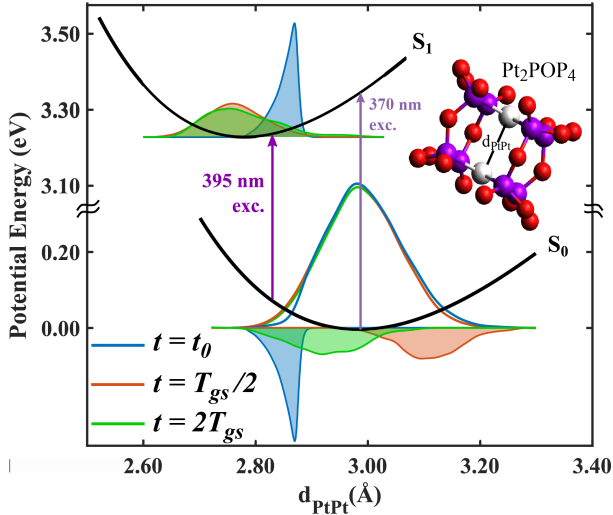
Figure 1. FIG. 1. Ground- and excited-state potential surfaces and QM/MM BOMD simulation of the structural dynamics following photoexcitation at 395 nm. The distribution of Pt-Pt distances is given by blue/red/green lines, representing the time steps $t = 0$, $t = T_{gs}/2$ and $t = 2T_{gs}$. An animation of the time evolution can be found in the SI.

the absorption band centered at 370 nm promotes an electron from the anti-bonding $5d\sigma^*$ HOMO orbital to the bonding $6p\sigma$ LUMO orbital [14]. Excitation to the $p\sigma$ orbital, located between the two Pt atoms, leads to a shortening of the Pt-Pt equilibrium distance from d_{PtPt}^{gs} =2.9-3.0 Å to d_{PtPt}^{es} =2.7-2.8 Å, with the bond shortening being closely similar in both the singlet (τ_{S_1} = 10-30 ps) and triplet (τ_{T_1} = 10 μs) excited states [15–18, 23]. Figure 1 shows the potential surfaces of the ground and S_1 excited state, the shape and positions of which determine the structural dynamics following photoexcitation. Excitation around $\lambda = 370$ nm leads to well-defined harmonic oscillations with period T^{es} close to 0.225 ps [19, 21, 23] as molecules near the bottom of the ground-state potential surface are promoted to S_1.

Low-temperature optical spectroscopy in the crystal phase [14] and Raman spectroscopy in solution [29, 30] determined the ground-state potential to be also highly harmonic but slightly softer than the singlet- and triplet-state potentials with a Pt-Pt oscillation with period T^{gs} = 0.285 ps. Whereas much effort has been devoted towards investigating the energy dissipation mechanisms and structural dynamics of the excited-state structure(s) of PtPOP [26, 31–33], no studies have directly addressed the ground-state dynamics. Here, we utilize off-resonance excitation at 395 nm to selectively excite solute molecules near the excited-state equilibrium geometry, see Figure 1.

To complement the experiments, the structural evolution following off-resonance excitation of PtPOP was also investigated via hybrid QM/MM BOMD simulations. Full descriptions of the methods are given in refer-

ences [25] and [26]. Briefly, PtPOP was modelled using DFT with the BLYP functional [34, 35], and a representation of the Kohn-Sham (KS) orbitals in terms of tzp basis set for the Pt atoms and dzp for the rest of the atoms [36]. The TIP4P force field [37] was used for the surrounding solvent. The simulations were realized using the BOMD code and QM/MM interfacing scheme [25] implemented in ASE [38, 39] and GPAW [40, 41].

To model the off-resonance excitation process, the simulation procedure first established a large set of ground-state configurations. From these, a subset with sufficiently short Pt-Pt distances to allow excitation to the singlet excited state by a 395 nm ($\approx$3.14 eV) photon was selected. Photoexcitation to the S_1 singlet state of PtPOP was modelled by starting 50 independent trajectories from this subset of ground-state configurations using the ΔSCF method [26, 42]. The procedure thus established two sets of trajectories, representing propagation of a depleted ground-state ensemble and of an excited-state ensemble. Figure 1 shows the d_{PtPt} distributions following the excitation event. We note that the semi-classical picture used to predict the dynamics taking place in the ground state after interaction with a short pump pulse implicitly incorporates effects that are commonly thought of as originating from a combination of absorption and impulsive stimulated Raman scattering [72].

Laser-pump/X-ray probe experiments were conducted at the LCLS facility. The XFEL delivered <50 fs 9.5 keV X-ray pulses at 120 Hz to the XPP experiment station [43], where the X-ray beam was focused to 30×30 μm^2. Laser excitation was by <50 fs 395(5) nm pulses, focused to a circular spot of <50 μm diameter and with a pulse energy of 3 μJ/pulse. The sample consisted of a 50 μm diameter free-flowing cylindrical jet of an 80 mM aqueous solution of PtPOP, with a flow speed sufficient to ensure full replenishment between pump/probe events. Scattered X-rays were detected by the 2D CSPAD [44] detector placed $\approx$5 cm behind the sample, allowing a Q-space coverage up to Q= 5 Å^{-1}, with $Q = \frac{4\pi}{\lambda}\sin(2\theta/2)$ where 2θ is the scattering angle and λ is the X-ray wavelength (1.31 Å). Following detector corrections, background subtraction and outlier rejection as previously described [45], 2D difference scattering images were constructed by subtracting laser-*off* images from laser-*on* images, where the laser had interacted with the sample at time t relative to the X-ray probe. Designating the scattering patterns with and without the excitation laser interacting with the sample as 'On' and 'Off' the difference signal is:

$$\Delta S(t) = S^{On}(t) - S^{Off} \qquad (1)$$

For the experiments and analysis described here, the individual difference scattering images were rebinned and subsequently averaged in 10 fs time bins according to the upstream Timing Tool [46] with approximately 150 images in each bin.

The contribution to the scattering patterns from the solute molecules is designated as either *gs* or *es* corresponding to ground- and excited-state molecules, the 'Off' signal is the scattering from just the ground-state equilibrium distribution of structures whereas the 'On'-signal arises from two contributions:

$$S^{\text{Off}} = S^{\text{gs,eq}};$$
$$S^{\text{On}}(t) = \alpha S^{\text{es}}(t) + (S^{\text{gs,eq}} - \alpha S^{\text{gs,hole}}(t)) \quad (2)$$

where α denotes the fraction of photoexcited PtPOP molecules in the probed sample volume at the given time delay. The term in the parentheses describes the population of ground-state molecules, of which the fraction α has been promoted to the excited state. The difference scattering signal is thus given by:

$$\Delta S(t) = \alpha[S^{\text{es}}(t) - S^{\text{gs,hole}}(t)] \quad (3)$$

As such, the acquired difference scattering signal arises from both the excited-state population as well as from the 'hole' that the excitation pulse created in the ground state.

The 2D difference images as acquired are anisotropic, with the anisotropic contribution to the scattering arising from preferential excitation of molecules with the transition dipole moment aligned parallel with the polarization of the excitation laser pulse. When the subsequent structural changes have a specific orientation with respect to the transition dipole moment, then the resulting scattering patterns will necessarily be anisotropic. This is the case here, as the $d\sigma^* p\sigma$ absorption peak has a transition dipole moment aligned along the Pt-Pt axis along which the Pt nuclei contract following photoexcitation. The difference scattering signal from such a distribution of solute molecules is described by [47, 48, 50]

$$\Delta S(Q,t) = \Delta S_0(Q,t) + P_2(\cos(\theta_q))\Delta S_2(Q,t); \quad (4)$$

-where the geometry of the experiment is introduced through θ_q, the angle between the laser polarization axis and $\mathbf{Q}$ with P_2 being a second-order Legendre polynomium.

Assuming that the solute in each of the vibrational ensembles *es* and *gs, hole* can be represented by a single average structure, the isotropic ΔS_0 and anisotropic ΔS_2 parts of the solute contributions to the difference scattering signal are calculated from [49, 50]:

$$S_0(Q) = \sum_{i,j}^{N} f_i(Q)f_j(Q)\frac{\sin(Qr_{ij})}{Qr_{ij}};$$
$$S_2(Q) = -c_2 \sum_{i,j}^{N} f_i(Q)f_j(Q)P_2(\cos(\xi_{ij}))j_2(r_{ij}); \quad (5)$$

-where we have suppressed the time-dependence for clarity of presentation. In these expressions, r_{ij} is the length
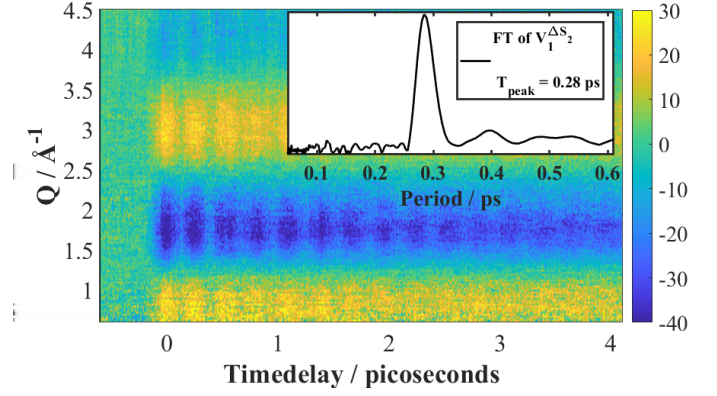

Figure 2. FIG. 2. $\Delta S_2(Q,t)$ with the color scale given in ‰-units of total signal. The inset shows the Fourier transform of the first right-singular vector of an SVD analysis, $|\mathcal{F}(V_1^{\Delta S_2})|$. A sharp peak at the T=0.28 ps ground-state period of PtPOP is observed.

of the vector $\mathbf{r_{ij}}$ connecting atoms i and j and ξ_{ij} is the angle between $\mathbf{r_{ij}}$ and the transition dipole moment of the molecule. j_2 the second-order spherical Bessel function and f_i refers to the form factor of atom i in the molecule consisting of N atoms. The time evolution of the orientational distribution is described by the pre-factor $c_2(t)$[50].

For the structural analysis presented here, the isotropic $\Delta S_0(Q)$ and anisotropic $\Delta S_2(Q)$ contributions to the difference signal were separated [48, 50]. The analysis presented below is focused on $\Delta S_2(Q,t)$, as this part of the full difference signal arises only from structural changes with a well-defined relationship to the excitation laser polarization axis and as such contains no contribution from the (isotropic) heating of the bulk solvent. The analysis of $\Delta S_0(Q,t)$ is shown in the SI, with key results reported in Figures 3 and 4.

Figure 2 shows $\Delta S_2(Q,t)$, where following photoexcitation at $t = 0$ a positive feature appears at low Q, indicative of a decrease in the average Pt-Pt distance in the probed sample volume. In the following picoseconds, the difference signal oscillates in intensity with little change in signal shape. Applying a Singular Value Decomposition to $\Delta S_2(Q,t)$ (SI), the inset shows the fourier transform of the time dependence of the acquired signal as described by the first right-singular vector of the difference signal, $|\mathcal{F}(V_1^{\Delta S_2})|$. From this, we find that structural dynamics of the photoexcited sample gives rise to a difference scattering signal exhibiting a pronounced oscillatory behavior with a period T close to 0.285 ps. This value is in very good agreement with the ground-state frequency of the Pt-Pt oscillations and significantly different from the $T = 0.210$-0.225 ps period of the singlet and triplet excited states [14, 19, 21]. From time-domain fourier transforms of ΔS_0 and ΔS_2 (SI), we estimate that contributions from excited-state dynamics (T=0.21-0.23 ps) to the observed difference signals is at most around 10%.

We ascribe this to two main factors: (i) off-resonance excitation, and (ii) within-pulse motion of the Pt nuclei smearing out the dynamics in the excited state more significantly than in the ground state. As such, photoexcitation at 395 nm preferentially excites the sub-population of PtPOP molecules with short Pt-Pt distances, that is, near the potential energy minimum of the singlet excited state (Figure 1). The photoexcited molecules therefore exhibit little or no coherent vibrational dynamics. Simultaneously, the ground-state population as characterized by the distribution of Pt-Pt distances is now no longer in equilibrium, as molecules with short Pt-Pt bond lengths have been preferentially excited. As the ensemble of molecules evolves, the ground-state population of molecules characterized at $t = 0$ by long Pt-Pt distances ($d_{\mathrm{PtPt}} \sim 3.1$ Å) will after $T^{\mathrm{gs}}/2$ have moved to short Pt-Pt distances, thus filling the 'hole' at $d_{\mathrm{PtPt}} = 2.77$ Å, which consequently moves to long Pt-Pt distances. In the following picoseconds, the hole propagates on the ground-state potential surface, eventually broadening to reflect the equilibrium ground-state distribution of Pt-Pt distances.

The difference signal $\Delta S(Q, t)$ was analyzed by structural fitting, employing a model incorporating a Pt-Pt distance-dependent depletion of the ground-state population as described above.

Within this analysis framework [17, 52], the excitation fraction and key structural parameters (here d_{PtPt}) are known to be strongly correlated [53]. To enable the robust determination of bond-length dynamics, the excitation fraction was first estimated by analyzing the difference signal at $t = 5$ ps where both the excited- and ground-state populations have reached their equilibrium distributions. The model applied in this step utilizes DFT-derived structures for the ground and excited state of PtPOP while maintaining the excitation fraction α as a free parameter. Obtaining a photoexcitation fraction $\alpha = 0.018(2)$, the second step of the structural analysis relies on locking this parameter in the analysis of the full data set. The difference signal modeling further assumes the excited-state population to have $d_{\mathrm{PtPt}} = 2.77$ Å for all time delays, while the ground-state distribution is assumed to be given by a combination of the ground-state equilibrium structure minus a hole characterized by a time-dependent Pt-Pt distance $d_{\mathrm{PtPt}}^{hole}(t)$. The model with which the observed time-dependent difference scattering signal was fit is thus:

$$\Delta S_2(Q, t) = \alpha[S_2^{\mathrm{es}}(Q) - S_2^{gs,hole}(Q, d_{\mathrm{PtPt}}^{hole}(t))] \quad (6)$$

-with all structural dynamics parameterized through the position of the ground-state hole, $d_{\mathrm{PtPt}}^{hole}(t)$ and with the scattering signals calculated through Eq. 5.

Figure 3 shows the fit at a representative time delay, $t = 0.25$ ps, and Figure 4A shows the best-fit value for d_{PtPt}^{hole} as a function of time delay t. d_{PtPt}^{hole} is observed to

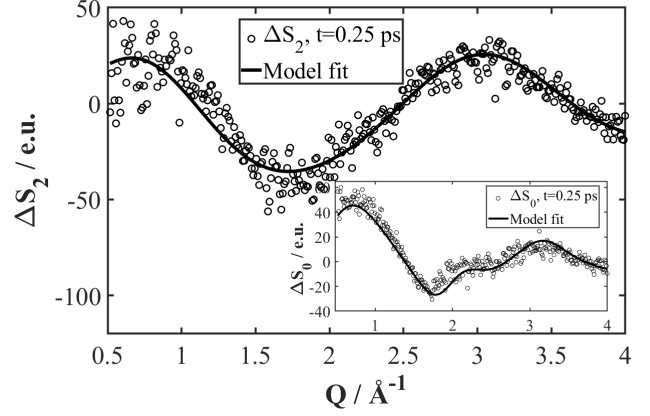Figure 3. FIG. 3. ΔS_2 and model fit at $t = 0.25$ ps after photoexcitation. Inset shows the corresponding fit of ΔS_0 at the same time delay.

move towards larger values immediately after excitation and then oscillates around the ground-state equilibrium distance in agreement with the discussion above. The time dependence is well described by an (IRF-broadened) exponentially damped sine function convoluted with a step function centered at $t = 0$. Fitting this function to $d_{\mathrm{PtPt}}^{hole}(t)$ we find a period $T^{hole} = 0.283(1)$ ps and decay time $\tau^{hole} = 2.2(2)$ ps.

Figure 4B shows the corresponding results of our QM/MM BOMD simulations. From these, we obtain a period of $T_{\mathrm{sim}}^{\mathrm{gs}} = 0.271$ ps, which agrees to within 5% with the experimental data. The decay of the oscillations takes place in $\tau_{gs,sim} = 0.7$ ps, which is three times faster than observed experimentally. We tentatively ascribe this difference as arising from the simulations overestimating the anharmonicity of the Pt-Pt potential. This is supported by the observation that the period of the simulated oscillations changes by around 20 fs from the first oscillation to the last, while no change can be discerned from the analysis of the experimental data.

The period and decay time of the observed oscillations derived from the ΔS_2 analysis, $T_{\mathrm{hole}}^{\mathrm{gs}} = 0.284(1)$ ps and $\tau = 2.2(2)$ ps, are in very good agreement with optical studies of PtPOP in ethylen glycole and in acetonitrile where $T^{\mathrm{gs}} = 0.281(3)$ ps and $\tau = 2.2(2)$ ps were found [19, 23]. The slightly faster decay time observed in the ΔS_0 analysis ($\tau = 1.7(3)$ ps) is likely spurious and arising from a small contribution from 2-photon excitation of PtPOP to $\Delta S_0(Q, t)$ as discussed in the SI.

The amplitude of the d_{PtPt}^{hole} oscillation is 0.06(1) Å, which is somewhat shorter than inferred from optical data [19] but in full agreement with the simulation result shown in Figure 4. The lower amplitude can thus be interpreted as due to the analysis tracking only the central position of the d_{PtPt}^{hole} distribution which rapidly broadens (Figure 1).
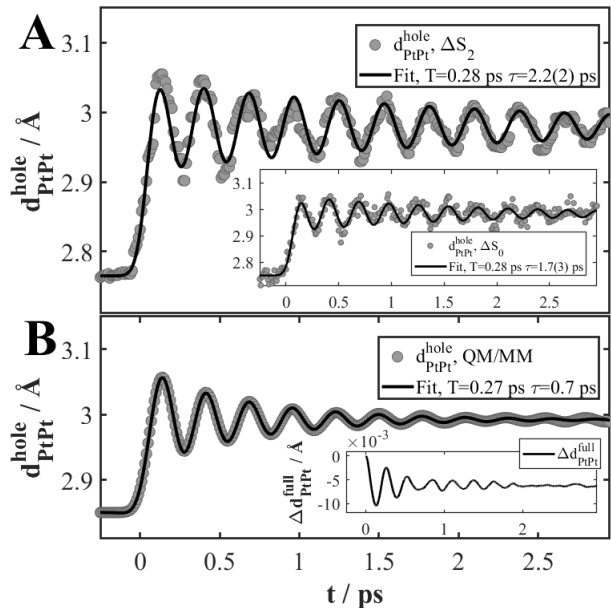
The results presented demonstrate the preparation of a

Figure 4. FIG. 4**A**: Time-dependent evolution of d_{PtPt}^{hole} (Gray circles). The dynamics have been fit (black line) with an IRF-broadened, exponentially damped sine function convoluted with a step function. Inset shows the ΔS_0 results. FIG. 4**B**: Time-dependent position of the hole (gray circles) from the simulations fitted with the same function (black line) as the experimental results. Inset shows the average Pt-Pt distance for the entire simulated ensemble.

vibrationally cold excited-state population and the evolution of a ground-state hole. Comparison with simulations allows direct and experimentally supported visualization of how the population distributions evolve on both the ground- and excited-state potential surfaces. Future experiments with better Q-space coverage will allow us to follow these dynamics in more detail, as recently discussed from a theoretical point of view [54] and experimentally realized for the Fe(bpy)$_3$ system using XAFS [55]. A key feature of the present experiment is the controlled preparation of a vibrationally cold excited state and we suggest that further studies utilizing vibrationally cold excited states may shed light on the temperature-dependent and highly elusive [22] mechanism of the singlet-triplet transition in PtPOP.

In summary, excitation with ultrashort optical laser pulses in combination with SASE-based X-ray laser sources can be used to prepare and track well-defined populations on the ground- and excited-state potential surfaces of molecules in solution. By choosing off-resonance excitation, the excited population can be prepared in a vibrationally cold state, allowing tracking of the ground-state dynamics alone.

[1] Thomas Elsaesser. Introduction: Ultrafast Processes in Chemistry. *CHEMICAL REVIEWS*, 117(16, SI):10621–10622, AUG 23 2017.

[2] Majed Chergui and Eric Collet. Photoinduced Structural Dynamics of Molecular Systems Mapped by Time-Resolved X-ray Methods. *CHEMICAL REVIEWS*, 117(16, SI):11025–11065, AUG 23 2017.

[3] Eric Collet and Marco Cammarata. Disentangling ultrafast electronic and structural dynamics with x-ray lasers. *Chemistry A European Journal*, 0(0), 2018.

[4] U. Banin, A. Bartana, S. Ruhman, and R. Kosloff. Impulsive excitation of coherent vibrational motion ground state surface dynamics induced by intense short pulses. *Journal of Chemical Physics*, 101(10):8461–8481, NOV 15 1994.

[5] E. Gershgoren, J. Vala, R. Kosloff, and S. Ruhman. Impulsive control of ground surface dynamics of I-3(-) in solution. *Journal of Physical Chemistry A*, 105(21):5081–5095, MAY 31 2001.

[6] A.M. Zheltikov. Coherent anti-Stokes Raman scattering: from proof-of-the-principle experiments to femtosecond CARS and higher order wave-mixing generalizations. *Journal of Raman Spectroscopy*, 31(8-9):653–667, AUG-SEP 2000.

[7] Robert W. Hartsock, Wenkai Zhang, Michael G. Hill, Bridgett Sabat, and Kelly J. Gaffney. Characterizing the Deformational Isomers of Bimetallic Ir$_2$(dimen)$_4^{2+}$ (dimen=1,8-diisocyano-p-menthane) with Vibrational Wavepacket Dynamics. *Journal of Physical Chemistry A*, 115(14):2920–2926, APR 14 2011.

[8] Renee R. Frontiera and Richard A. Mathies. Femtosecond stimulated Raman spectroscopy. *Laser & Photonics Reviews*, 5(1):102–113, JAN 2011.

[9] Th. Ergler, B. Feuerstein, A. Rudenko, K. Zrost, C. D. Schroeter, R. Moshammer, and J. Ullrich. Quantum-phase resolved mapping of ground-state vibrational D-2 wave packets via selective depletion in intense laser pulses. *Physical Review Letters*, 97(10), SEP 8 2006.

[10] Erich Goll, Gunter Wunner, and Alejandro Saenz. Formation of ground-state vibrational wave packets in in-

tense ultrashort laser pulses. *Physical Review Letters*, 97(10), SEP 8 2006.

[11] L. Fang and G. N. Gibson. Strong-field induced vibrational coherence in the ground electronic state of hot I(2). *Physical Review Letters*, 100(10), MAR 14 2008.

[12] Johann Foerster, Etienne Plesiat, Alvaro Magana, and Alejandro Saenz. Imaging of the umbrella motion and tunneling in ammonia molecules by strong-field ionization. *Physical Review A*, 94(4), OCT 5 2016.

[13] Christoph Bostedt, Sebastien Boutet, David M. Fritz, Zhirong Huang, Hae Ja Lee, Henrik T. Lemke, Aymeric Robert, William F. Schlotter, Joshua J. Turner, and Garth J. Williams. Linac Coherent Light Source: The first five years. *Reviews of Modern Physics*, 88(1), MAR 9 2016.

[14] S.F. Rice and H.B. Gray. Electronic absorption and emission spectra of binuclear platinum(II) complexes - characterization of the lowest singlet and triplet excited states of $Pt_2(H_2P_2O_5)_4{}^{4-}$. *Journal of the American Chemical Society*, 105(14):4571–4575, 1983.

[15] C.D. Kim, S. Pillet, G. Wu, W.K. Fullagar, and P. Coppens. Excited-state structure by time-resolved X-ray diffraction. *Acta Crystallographica Section A*, 58(2):133–137, MAR 2002.

[16] N. Yasuda, M. Kanazawa, H. Uekusa, and Y. Ohashi. Excited-state structure of a platinum complex by X-ray analysis. *Chemistry Letters*, pages 1132–1133, NOV 5 2002.

[17] Morten Christensen, Kristoffer Haldrup, Klaus Bechgaard, Robert Feidenhans'l, Qingyu Kong, Marco Cammarata, Manuela Lo Russo, Michael Wulff, Niels Harrit, and Martin Meedom Nielsen. Time-Resolved X-ray Scattering of an Electronically Excited State in Solution. Structure of the (3)A(2u) State of Tetrakis-mu-pyrophosphitodiplatinate(II). *Journal of the American Chemical Society*, 131(2):502–508, JAN 21 2009.

[18] Renske M. van der Veen, Chris J. Milne, Amal El Nahhas, Frederico A. Lima, Van-Thai Pham, Jonathan Best, Julia A. Weinstein, Camelia N. Borca, Rafael Abela, Christian Bressler, and Majed Chergui. Structural Determination of a Photochemically Active Diplatinum Molecule by Time-Resolved EXAFS Spectroscopy. *Angewandte Chemie - International Edition*, 48(15):2711–2714, 2009.

[19] Renske M. van der Veen, Andrea Cannizzo, Frank van Mourik, Antonin Vlcek, Jr., and Majed Chergui. Vibrational Relaxation and Intersystem Crossing of Binuclear Metal Complexes in Solution. *Journal of the American Chemical Society*, 133(2):305–315, JAN 19 2011.

[20] Marc-Oliver Winghart, Ji-Ping Yang, Matthias Vonderach, Andreas-Neil Unterreiner, Dao-Ling Huang, Lai-Sheng Wang, Sebastian Kruppa, Christoph Riehn, and Manfred M. Kappes. Time-resolved photoelectron spectroscopy of a dinuclear Pt(II) complex: Tunneling autodetachment from both singlet and triplet excited states of a molecular dianion. *Journal of Chemical Physics*, 144(5), FEB 7 2016.

[21] Roberto Monni, Gerald Aubck, Dominik Kinschel, Kathrin M. Aziz-Lange, Harry B. Gray, Antonn Vlek, and Majed Chergui. Conservation of vibrational coherence in ultrafast electronic relaxation: The case of diplatinum complexes in solution. *Chemical Physics Letters*, pages –, 2017.

[22] Harry B. Gray, Stanislav Zalis, and Antonin Vlcek. Electronic structures and photophysics of d(8)-d(8) com-

plexes. *Coordination Chemistry Reviews*, 345:297–317, AUG 15 2017.

[23] Roberto Monni, Gloria Capano, Gerald Auböck, Harry B. Gray, Antonín Vlček, Ivano Tavernelli, and Majed Chergui. Vibrational coherence transfer in the ultrafast intersystem crossing of a diplatinum complex in solution. *Proceedings of the National Academy of Sciences*, 2018.

[24] Asmus Ougaard Dohn, Elvar Örn Jonsson, Kasper Skov Kjær, Tim Brandt van Driel, Martin Meedom Nielsen, Karsten Wedel Jacobsen, Niels Engholm Henriksen, and Klaus Braagaard Møller. Direct Dynamics Studies of a Binuclear Metal Complex in Solution: The Interplay Between Vibrational Relaxation, Coherence, and Solvent Effects. *Journal of Physical Chemistry Letters*, 5(14):2414–2418, JUL 17 2014.

[25] A. O. Dohn, Elvar Örn Jonsson, G. Levi, J. J. Mortensen, O. Lopez-Acevedo, K. S. Thygesen, K. W. Jacobsen, J. Ulstrup, N. E. Henriksen, K. B. Møller, and H. Jonsson. Grid-based projector augmented wave (gpaw) implementation of quantum mechanics/molecular mechanics (qm/mm) electrostatic embedding and application to a solvated diplatinum complex. *Journal of Chemical Theory and Computation*, 13(12):6010–6022, 2017. PMID: 29083921.

[26] Gianluca Levi, Matyas Papai, Niels E. Henriksen, Asmus O. Dohn, and Klaus B. Møller. Solution Structure and Ultrafast Vibrational Relaxation of the PtPOP Complex Revealed by Delta SCF-QM/MM Direct Dynamics Simulations. *Journal of Physical Chemistry C*, 122(13):7100–7119, APR 5 2018.

[27] DM Jonas, SE Bradforth, SA Passino, and GR Fleming. Femtosecond wavepacket spectroscopy - influence of temperature, wavelength and pulse duration. *Journal of Physical Chemistry*, 99(9):2594–2608, MAR 2 1995.

[28] Donald A. McQuarrie. *Statistical Mechanics*. Harper & Row, 1975.

[29] C.M. Che, F.H. Herbstein, W.P. Schaeffer, R.E. Marsh, and H.B. Gray. Binuclear platinum diphosphite complexes - crystal-structures of $K_4[Pt_2(POP)_4Br]$-$3H_2O$, a new linear-chain semiconductor, and $K_4[Pt_2(POP)_4Cl_2]$-$2H_2O$. *Journal of the American Chemical Society*, 105(14):4604–4607, 1983.

[30] K.H. Leung, D.L. Phillips, C.M. Che, and V.M. Miskowski. Resonance Raman intensity analysis investigation of metal-metal bonded transitions: an examination of the $_1A^{2u}$ ¡- $_1A^{1g}$ (5d σ^* -¿ 6p σ) transition of $Pt_2(H_2P_2O_5)_4{}^{4-}$. *Journal of Raman Spectroscopy*, 30(11):987–993, NOV 1999.

[31] Alec C. Durrell, Gretchen E. Keller, Yan-Choi Lam, Jan Sykora, Antonin Vlcek, Jr., and Harry B. Gray. Structural Control of (1)A(2u)-to-(3)A(2u) Intersystem Crossing in Diplatinum(II,II) Complexes. *Journal of the American Chemical Society*, 134(34):14201–14207, AUG 29 2012.

[32] Stanislav Zalis, Yan-Choi Lam, Harry B. Gray, and Antonin Vlcek. Spin-Orbit TDDFT Electronic Structure of Diplatinum(II,II) Complexes. *Inorganic Chemistry*, 54(7):3491–3500, APR 6 2015.

[33] Yan Choi Lam, Harry B. Gray, and Jay R. Winkler. Intersystem Crossing in Diplatinum Complexes. *Journal of Physical Chemistry A*, 120(39):7671–7676, OCT 6 2016.

[34] A. D. Becke. Density-functional exchange-energy approximation with correct asymptotic behavior. *Physical Review A*, 38:3098, 1988.

[35] C. Lee, W. Yang, and R. G. Parr. Development of the colle-salvetti correlation-energy formula into a functional of the electron density. *Physical Review B*, 37:785–789, 1988.

[36] A. H. Larsen, M. Vanin, J. J. Mortensen, K. S. Thygesen, and K. W. Jacobsen. Localized atomic basis set in the projector augmented wave method. *Phys. Rev. B*, 80:195112, 2009.

[37] W. L. Jorgensen. Quantum and statistical mechanical studies of liquids. 10. transferable intermolecular potential functions for water, alcohols, and ethers. application to liquid water. *Journal of the American Chemical Society*, 103:335–340, 1981.

[38] S. R. Bahn and K. W. Jacobsen. An object-oriented scripting interface to a legacy electronic structure code. *Computing in Science & Engineering*, 4:55, 2002.

[39] Ask Hjorth Larsen, Jens Jørgen Mortensen, Jakob Blomqvist, Ivano E Castelli, Rune Christensen, Marcin Dułak, Jesper Friis, Michael N Groves, Bjørk Hammer, Cory Hargus, Eric D Hermes, Paul C Jennings, Peter Bjerre Jensen, James Kermode, John R Kitchin, Esben Leonhard Kolsbjerg, Joseph Kubal, Kristen Kaasbjerg, Steen Lysgaard, Jón Bergmann Maronsson, Tristan Maxson, Thomas Olsen, Lars Pastewka, Andrew Peterson, Carsten Rostgaard, Jakob Schiøtz, Ole Schütt, Mikkel Strange, Kristian S Thygesen, Tejs Vegge, Lasse Vilhelmsen, Michael Walter, Zhenhua Zeng, and Karsten W Jacobsen. The atomic simulation environmenta python library for working with atoms. *Journal of Physics: Condensed Matter*, 29(27):273002, 2017.

[40] J.J. Mortensen, L.B. Hansen, and K. W. Jacobsen. Real-space grid implementation of the projector augmented wave method. *Physical Review B*, 71:035109, 2005.

[41] J. Enkovaara, C. Rostgaard, J. J. Mortensen, J. Chen, M. Dulak, L. Ferrighi, J. Gavnholt, C. Glinsvad, V. Haikola, H. A. Hansen, H. H. Kristoffersen, M. Kuisma, A. H. Larsen, L. Lehtovaara, M. Ljungberg, O. Lopez-Acevedo, P. G. Moses, J. Ojanen, T. Olsen, V. Petzold, N. A. Romero, J. Stausholm-Møller, M. Strange, G. A. Tritsaris, M. Vanin, M. Walter, B. Hammer, H. H.äkkinen, G. K. H. Madsen, R. M. Nieminen, J. K. Nørskov, M. Puska, T. T. Rantala, J. Schiøtz, K. S. Thygesen, and K. W. Jacobsen. Electronic structure calculations with gpaw: a real-space implementation of the projector augmented-wave method. *Journal of Physics: Condensed matter*, 22:253202, 2010.

[42] Jeppe Gavnholt, Thomas Olsen, Mads Engelund, and Jakob Schiotz. Delta self-consistent field method to obtain potential energy surfaces of excited molecules on surfaces. *Physical Review B*, 78(7), AUG 2008.

[43] Matthieu Chollet, Roberto Alonso-Mori, Marco Cammarata, Daniel Damiani, Jim Defever, James T. Delor, Yiping Feng, James M. Glownia, J. Brian Langton, Silke Nelson, Kelley Ramsey, Aymeric Robert, Marcin Sikorski, Sanghoon Song, Daniel Stefanescu, Venkat Srinivasan, Diling Zhu, Henrik T. Lemke, and David M. Fritz. The X-ray Pump-Probe instrument at the Linac Coherent Light Source. *Journal of Synchrotron Radiation*, 22(3, SI):503–507, MAY 2015.

[44] Hugh T. Philipp, Marianne Hromalik, Mark Tate, Lucas Koerner, and Sol M. Gruner. Pixel array detector for X-ray free electron laser experiments. *Nuclear Instruments & Methods in Physics Research Section A - Accelerators, Spectrometers, Detectors and associated equipment*, 649(1):67–69, SEP 1 2011. 16th Pan-American Conference on Synchrotron Radiation Instrumentation (SRI2010), Chicago, IL, SEP 21-24, 2010.

[45] Tim Brandt van Driel, Kasper Skov Kjaer, Elisa Biasin, Kristoffer Haldrup, Henrik Till Lemke, and Martin Meedom Nielsen. Disentangling detector data in XFEL studies of temporally resolved solution state chemistry. *Faraday Discussions*, 177:443–465, 2015.

[46] M. Harmand, R. Coffee, M. R. Bionta, M. Chollet, D. French, D. Zhu, D. M. Fritz, H. T. Lemke, N. Medvedev, B. Ziaja, S. Toleikis, and M. Cammarata. Achieving few-femtosecond time-sorting at hard X-ray free-electron lasers. *Nature Photonics*, 7(3):215–218, MAR 2013.

[47] J. Spencer Baskin and Ahmed H. Zewail. Oriented ensembles in ultrafast electron diffraction. *ChemPhysChem*, 7(7):1562–1574, JUL 17 2006.

[48] U. Lorenz, K. B. Møller, and N. E. Henriksen. On the interpretation of time-resolved anisotropic diffraction patterns. *New Journal of Physics*, 12, NOV 10 2010.

[49] Asmus O. Dohn, Elisa Biasin, Kristoffer Haldrup, Martin M. Nielsen, Niels E. Henriksen, and Klaus B. Møller. On the calculation of x-ray scattering signals from pairwise radial distribution functions (vol 48, 244010, 2015). *Journal of Physics B - Atomic, Molecular and Optical Physics*, 49(5), MAR 14 2016.

[50] Elisa Biasin, Tim B. van Driel, Gianluca Levi, Mads G. Laursen, Asmus O. Dohn, Asbjorn Moltke, Peter Vester, Frederik B. K. Hansen, Kasper S. Kjaer, Tobias Harlang, Robert Hartsock, Morten Christensen, Kelly J. Gaffney, Niels E. Henriksen, Klaus B. Møller, Kristoffer Haldrup, and Martin M. Nielsen. Anisotropy enhanced X-ray scattering from solvated transition metal complexes. *Journal of Synchrotron Radiation*, 25(2):306–315, MAR 2018.

[51] Elisa Biasin, Tim Brandt van Driel, Kasper S. Kjaer, Asmus O. Dohn, Morten Christensen, Tobias Harlang, Pavel Chabera, Yizhu Liu, Jens Uhlig, Matyas Papai, Zoltan Nemeth, Robert Hartsock, Winnie Liang, Jianxin Zhang, Roberto Alonso-Mori, Matthieu Chollet, James M. Glownia, Silke Nelson, Dimosthenis Sokaras, Tadesse A. Assefa, Alexander Britz, Andreas Galler, Wojciech Gawelda, Christian Bressler, Kelly J. Gaffney, Henrik T. Lemke, Klaus B. Møller, Martin M. Nielsen, Villy Sundstrom, Gyorgy Vanko, Kenneth Warnmark, Sophie E. Canton, and Kristoffer Haldrup. Femtosecond X-Ray Scattering Study of Ultrafast Photoinduced Structural Dynamics in Solvated $[Co(terpy)_2]^{2+}$. *Physical Review Letters*, 117(1), JUN 30 2016.

[52] Kristoffer Haldrup, Tobias Harlang, Morten Christensen, Asmus Dohn, Tim Brandt van Driel, Kasper Skov Kjaer, Niels Harrit, Johan Vibenholt, Laurent Guerin, Michael Wulff, and Martin Meedom Nielsen. Bond Shortening (1.4 angstrom) in the Singlet and Triplet Excited States of $[Ir_2(dimen)_4]^{2+}$ in Solution Determined by Time-Resolved X-ray Scattering. *Inorganic Chemistry*, 50(19):9329–9336, OCT 3 2011.

[53] Kristoffer Haldrup, Morten Christensen, and Martin Meedom Nielsen. Analysis of time-resolved X-ray scattering data from solution-state systems. *Acta Crystallographica Section A*, 66(2):261–269, MAR 2010.

[54] Adam Kirrander and Peter M. Weber. Fundamental Limits on Spatial Resolution in Ultrafast X-ray Diffraction. *Applied Sciences*, 7(6), JUN 2017.

[55] Henrik T. Lemke, Kasper S. Kjaer, Robert Hartsock, Tim B. van Driel, Matthieu Chollet, James M. Glownia, Sanghoon Song, Diling Zhu, Elisabetta Pace, Samir F. Matar, Martin M. Nielsen, Maurizio Benfatto, Kelly J. Gaffney, Eric Collet, and Marco Cammarata. Coherent structural trapping through wave packet dispersion during photoinduced spin state switching. *Nature Communications*, 8, MAY 24 2017.

[56] Supplemental Material is available with this manuscript and includes Refs. [57–81]

[57] C.M. Che, L.G. Butler, P.J. Grunthaner, and H.B. Gray. Chemistry and spectroscopy of binuclear diplatinum complexes. *Inorganic Chemistry*, 24(26):4662–4665, DEC 18 1985.

[58] Kasper Skov Kjær, Tim B. van Driel, Jan Kehres, Kristoffer Haldrup, Dmitry Khakhulin, Klaus Bechgaard, Marco Cammarata, Michael Wulff, Thomas Just Sorensen, and Martin M. Nielsen. Introducing a standard method for experimental determination of the solvent response in laser pump, X-ray probe time-resolved wide-angle X-ray scattering experiments on systems in solution. *Physical Chemistry Chemical Physics*, 15(36):15003–15016, 2013.

[59] Kristoffer Haldrup, Wojciech Gawelda, Rafael Abela, Roberto Alonso-Mori, Uwe Bergmann, Amelie Bordage, Marco Cammarata, Sophie E. Canton, Asmus O. Dohn, Tim Brandt van Driel, David M. Fritz, Andreas Galler, Pieter Glatzel, Tobias Harlang, Kasper S. Kjaer, Henrik T. Lemke, Klaus B. Møller, Zoltan Nemeth, Matyas Papai, Norbert Sas, Jens Uhlig, Diling Zhu, Gyoergy Vanko, Villy Sundstroem, Martin M. Nielsen, and Christian Bressler. Observing Solvation Dynamics with Simultaneous Femtosecond X-ray Emission Spectroscopy and X-ray Scattering. *Journal of Physical Chemistry B*, 120(6):1158–1168, FEB 18 2016.

[60] J.R. Peterson and K. Kalyanasundaram. Energy-transfer and electron-transfer processes of the lowest triplet excited-state of tetrakis(diphosphito)diplatinate(II). *Journal of Physical Chemistry*, 89(12):2486–2492, 1985.

[61] Denis Leshchev, Tobias C. B. Harlang, Lisa A. Fredin, Dmitry Khakhulin, Yizhu Liu, Elisa Biasin, Mads G. Laursen, Gemma E. Newby, Kristoffer Haldrup, Martin M. Nielsen, Kenneth Warnmark, Villy Sundstrom, Petter Persson, Kasper S. Kjaer, and Michael Wulff. Tracking the picosecond deactivation dynamics of a photoexcited iron carbene complex by time-resolved X-ray scattering. *Chemical Science*, 9(2):405–414, JAN 14 2018.

[62] A.E. Stiegman, S.F. Rice, H.B. Gray, and V.M. Miskowski. Electronic spectroscopy of diplatinum complexes - excited states of $Pt_2(P_2O_5H_2)_4^{4-}$. *Inorganic Chemistry*, 26(7):1112–1116, APR 8 1987.

[63] S. R. Bahn and K. W. Jacobsen. An object-oriented scripting interface to a legacy electronic structure code. *Computing in Science & Engineering*, 4:55, 2002.

[64] A. H. Larsen, J. J. Mortensen, J. Blomqvist, I. E. Castelli, R. Christensen, M. Dułak, J. Friis, M. N. Groves, B. Hammer, C. Hargus, E. D. Hermes, P. C. Jennings, P. B. Jensen, J. Kermode, J. R. Kitchin, E. L. Kolsbjerg, J. Kubal, K. Kaasbjerg, S. Lysgaard, J. B. Maronsson, T. Maxson, T. Olsen, L. Pastewka, A. Peterson, C. Rostgaard, J. Schiøtz, O. Schütt, M. Strange, K. S. Thygesen, T. Vegge, L. Vilhelmsen, M. Walter, Z. Zeng, and K. W. Jacobsen. The atomic simulation environmenta python library for working with atoms. *Journal of Physics: Condensed Matter*, 29(27):273002, 2017.

[65] J. J. Mortensen, L. B. Hansen, and K. W. Jacobsen. Real-space grid implementation of the projector augmented wave method. *Physical Review B*, 71:035109, 2005.

[66] J. Enkovaara, C. Rostgaard, J. J. Mortensen, J. Chen, M. Dulak, L. Ferrighi, J. Gavnholt, C. Glinsvad, V. Haikola, H. A. Hansen, H. H. Kristoffersen, M. Kuisma, A. H. Larsen, L. Lehtovaara, M. Ljungberg, O. Lopez-Acevedo, P. G. Moses, J. Ojanen, T. Olsen, V. Petzold, N. A. Romero, J. Stausholm-Møller, M. Strange, G. A. Tritsaris, M. Vanin, M. Walter, B. Hammer, H. Häkkinen, G. K. H. Madsen, R. M. Nieminen, J. K. Nørskov, M. Puska, T. T. Rantala, J. Schiøtz, K. S. Thygesen, and K. W. Jacobsen. Electronic structure calculations with gpaw: a real-space implementation of the projector augmented-wave method. *Journal of Physics: Condensed matter*, 22:253202, 2010.

[67] A. H. Larsen, M. Vanin, J. J. Mortensen, K. S. Thygesen, and K. W. Jacobsen. Localized atomic basis set in the projector augmented wave method. *Phys. Rev. B*, 80:195112, 2009.

[68] A. D. Becke. Density-functional exchange-energy approximation with correct asymptotic behavior. *Physical Review A*, 38:3098, 1988.

[69] C. Lee, W. Yang, and R. G. Parr. Development of the colle-salvetti correlation-energy formula into a functional of the electron density. *Physical Review B*, 37:785–789, 1988.

[70] G. Levi. *Photoinduced Molecular Dynamics in Solution*. PhD thesis, Technical University of Denmark, 2018.

[71] W. L. Jorgensen, J. Chandrasekhar, J. D. Madura, R. W. Impey, and M. L. Klein. Comparison of simple potential functions for simulating liquid water. *Journal of Chemical Physics*, 79:926–935, 1983.

[72] DM Jonas, SE Bradforth, SA Passino, and GR Fleming. Femtosecond wavepacket spectroscopy - influence of temperature, wavelength and pulse duration. *Journal of Physical Chemistry*, 99(9):2594–2608, MAR 2 1995.

[73] A.K. Rappe, C.J. Casewit, K.S. Colwell, W.A. Goddard III, and W.M. Skiff. Uff, a full periodic table force field for molecular mechanics and molecular dynamics simulations. *Journal of the American Chemical Society*, 114:10024–10035, 1992.

[74] H. C. Andersen. Rattle: A "velocity" version of the shake algorithm for molecular dynamics calculations. *Journal of Computational Physics*, 52:24, 1983.

[75] J. Petersen, N. E. Henriksen, and K. B. Møller. Validity of the Bersohn-Zewail model beyond justification. *Chemical Physics Letters*, 539-540:234–238, 2012.

[76] Klaus B. Møller, Rossend Rey, and James T. Hynes. Hydrogen bond dynamics in water and ultrafast infrared spectroscopy: A theoretical study. *Journal of Physical Chemistry A*, 108:1275–1289, 2004.

[77] V. A. Ermoshin and V. Engel. Femtosecond pump-probe fluorescence signals from classical trajectories: Comparison with wave-packet calculations. *European Physical Journal D*, 15:413–422, 2001.

[78] Z. Li, J.-Y. Fang, and C. C. Martens. Simulation of ultrafast dynamics and pump-probe spectroscopy using classical trajectories. *The Journal of Chemical Physics*,

104(18):6919, 1996.

[79] E.H. Van Kleef and I. Powis. Anisotropy in the preparation of symmetric top excited states. I. One-photon electric dipole excitation. *Molecular Physics*, 96(5):757–774, 1999.

[80] Reinhard J. Maurer and Karsten Reuter. Assessing computationally efficient isomerization dynamics: ΔSCF density-functional theory study of azobenzene molecular switching. *Journal of Chemical Physics*, 135(22):224303, 2011.

[81] Burak Himmetoglu, Alex Marchenko, Isma??la Dabo, and Matteo Cococcioni. Role of electronic localization in the phosphorescence of iridium sensitizing dyes. *Journal of Chemical Physics*, 137(15):154309, 2012.

[82] D. A. McQuarrie. *Statistical Mechanics*. Harper & Row, 1976.